

A new method to measure the virial factors in the reverberation mapping of AGNs

H. T. Liu^{1,3*}, H. C. Feng^{1,2,3} and J. M. Bai^{1,3}

¹Yunnan Observatories, Chinese Academy of Sciences, Kunming, Yunnan 650011, China

²University of Chinese Academy of Sciences, Beijing 100049, China

³Key Laboratory for the Structure and Evolution of Celestial Objects, Chinese Academy of Sciences, Kunming, Yunnan 650011, China

Accepted . Received

ABSTRACT

Based on the gravitational redshift, one prediction of Einstein's general relativity theory, of broad optical emission lines in active galactic nuclei (AGNs), a new method is proposed to estimate virial factors f in reverberation mapped masses of black holes M_{RM} . The factors f can be measured on the basis of two physical quantities, i.e. gravitational redshifts z_g and full widths at half maxima ($FWHM$ s) of broad lines. The factors f are difficult to be determined due to the unclear kinematics and geometry of broad-line regions (BLRs) in AGNs. This new method is applied to narrow-line Seyfert 1 galaxy (NLS1) Mrk 110. The factor f increases with the increasing BLR size for the gravitationally redshifted broad lines He II, He I, $H\beta$ and $H\alpha$ in Mrk 110. This trend likely results from the radiation pressure influence of accretion disc on the BLR clouds. The radiation pressure influence seems to be more important than thought usually in AGNs. Mrk 110 has $f \approx 8\text{--}16$ that are distinctly larger than the mean $\langle f \rangle \approx 1$ usually used to estimate M_{RM} in the case of $FWHM$. These larger f values will produce higher M_{RM} and lower Eddington ratios. **$f = 2.9$ is derived for Seyfert 1 galaxy NGC 4593. Higher f of several tens are derived for other three mapped NLS1s. The larger factor f corresponds to the higher accretion rate for NGC 4593, Mrk 110 and other two NLS1s.** The high- f values of NLS1s suggest that their BLRs are nearly face-on viewed if BLRs are disc-like.

Key words: black hole physics – galaxies: active – galaxies: nuclei – galaxies: Seyfert – quasars: emission lines.

1 INTRODUCTION

Active galactic nuclei (AGNs), such as quasars and Seyfert galaxies, can be powered by the releases of gravitational potential energy of accretion of matter onto supermassive black holes surrounded by accretion discs (Rees et al. 1982; Rees 1984). The reverberation mapping model shows that the broad emission line variations are driven by the ionizing continuum variations through the photoionization process (e.g. Blandford & McKee 1982; Peterson 1993). **Broad-line region (BLR) radius r_{BLR} can be determined by time lag τ between the broad-line and continuum variations, as $r_{\text{BLR}} = \tau c$, where c is the speed of light.** The reverberation mapping observations and researches have been carried out for AGNs over the last several decades (e.g. Kaspi & Netzer 1999; Kaspi et al. 2000, 2007; Peterson et al. 2005; Denney et al. 2010; Haas et al. 2011; Pozo Nuñez et al. 2012; Du et al.

2014, 2015; Pei et al. 2014; Wang et al. 2014; Barth et al. 2015; Hu et al. 2015). Recently, some reverberation mapping surveys are proposed and carried out, such as the Sloan Digital Sky Survey (SDSS) spectroscopic reverberation mapping project (Shen et al. 2015a,b, 2016) and the OzDES AGN spectroscopic reverberation mapping project (King et al. 2015). Thus, the reverberation mapping studies will be the most efficient method to estimate the black hole masses of AGNs. However, the virial factors f in the reverberation mapping mass estimation are uncertain due to the unclear kinematics and geometry of BLRs in AGNs (Peterson et al. 2004; Woo et al. 2015). The range of f appears to span several orders of magnitude (e.g. Woo & Urry 2002). An average $\langle f \rangle \approx 1$ is derived on the basis of black hole mass–stellar velocity dispersion relation ($M_{\bullet} - \sigma_{\star}$ relation) for the low redshift quiescent galaxies and/or reverberation mapped AGNs using the full widths at half maxima ($FWHM$ s) of Balmer emission lines (Onken et al. 2004; Piotrovich et al. 2015; Woo et al. 2015). Constraining the

* E-mail: htliu@ynao.ac.cn

virial factor f is an important task for investigating black hole mass related issues.

The BLR cloud motions of the reverberation mapped AGNs are believed and/or assumed to be dominated by the gravitational forces of the central supermassive black holes (i.e. virialized motions) (e.g. Krolik et al. 1991; Wandel et al. 1999; Krolik 2001; Barth et al. 2011; Du et al. 2014; Wang et al. 2014). Their motions generate the observed *FWHM*s of optical broad emission lines, typically thousands of km s^{-1} . The optical BLRs usually span from hundreds to thousands of gravitational radii from the central black holes for the reverberation mapped AGNs. At the huge distances, the broad lines should be redshifted due to the gravity of the central black hole. Gravitational redshift in the weak field regime establishes pure shifts of spectral features without changing their intrinsic shapes and in the strong field regime produces remarkable distortions of spectral shapes (Müller & Wold 2006). Remarkable profile distortion is a key feature of relativistic spectra of AGNs with very skewed and asymmetric line profiles, e.g. iron $\text{K}\alpha$ lines, generated in the emitting regions very close to the central black holes (e.g. Fabian et al. 1989; Popovic et al. 1995; Tanaka et al. 1995; Fabian et al. 2000; Reynolds & Nowak 2003). There are three ways to measure the gravitational redshift. First, it is measured for a broad line as a redshift difference with respect to $[\text{O III}] \lambda 5007$ (e.g. Zheng & Sulentic 1990; McIntosh et al. 1999b; Tremaine et al. 2014). Second, it is measured at different levels of the line intensity as a centroid shift with respect to the broad line peak (Jonić et al. 2016). Third, it is measured as a broad-line centroid difference between the mean spectrum and the root mean square (rms) spectrum (Kollatschny 2003b). Tremaine et al. (2014) intensively studied the gravitational redshift of broad $\text{H}\beta$ for over 20,000 quasars in the SDSS Data Release 7 (DR7). The gravitational redshift is detected in a statistical sense for the single-epoch spectra. The $\text{H}\beta$ mean shift increases as *FWHM* increases for these quasars. Jonić et al. (2016) found a positive correlation between intrinsic redshifts dominantly caused by the gravitational effect and widths of $\text{H}\beta$ for 209 AGNs taken from the SDSS DR7. According to the virial assumption, the BLR radius is inversely proportional to the square of *FWHM*. So, the $\text{H}\beta$ shift will increase with the decreasing radius of BLR, i.e. the gravitational redshifts of the broad lines will be larger as their BLRs become closer to the central black holes.

The reverberation mapped black hole masses are $M_{\text{RM}} \sim 10^6\text{--}10^7 M_{\odot}$ for Seyfert 1 galaxies (e.g. Kaspi & Netzer 1999; Kaspi et al. 2000; Peterson et al. 2005; Bentz et al. 2006; Denney et al. 2010; Haas et al. 2011; Du et al. 2014, 2015; Wang et al. 2014). Seyfert 1 galaxies have a relatively high Eddington ratio $L_{\text{bol}}/L_{\text{Edd}}$, where L_{bol} is the bolometric luminosity and L_{Edd} is the Eddington luminosity. Narrow-line Seyfert 1 galaxies (NLS1s) seem to have a more high Eddington ratio. Some NLS1s are accreting at super-Eddington accretion state. A large reverberation mapping campaign was performed by the

Yunnan Observatory 2.4 m telescope from 2012 to 2013 for AGNs with super-Eddington accreting massive black holes (SEAMBHs) (Du et al. 2014; Wang et al. 2014). Hu et al. (2015) studied the properties of emission lines for 10 NLS1s with SEAMBHs, and found the redshifts and blueshifts of $\text{H}\beta$ and Fe II . The inflow and outflow of BLR clouds could generate these redshifts and blueshifts, respectively. Kollatschny (2003a) ruled out that radial inflow or outflow motions are dominant in the BLR of Seyfert 1 galaxy Mrk 110. The $\text{H}\beta$ line in Seyfert 1 galaxy Mrk 50 has an origin in a BLR dominated by orbital motion rather than infall or outflow (Barth et al. 2011). Kollatschny (2003b) found the gravitationally redshifted broad emission lines He II , He I , $\text{H}\beta$ and $\text{H}\alpha$. The BLRs will "breathe" with the central radiation variations (e.g. Barth et al. 2015, references therein). The breaths occur on short timescales of days to weeks in response to continuum variations, and the broad-line velocity shifts are of the order of 100 km s^{-1} over about one month. The breath effects of BLRs on the broad-line shifts may be eliminated in the rms and mean spectra of the reverberation mapped AGNs. The gravitational redshifts of the broad lines in Mrk 110 were determined based on the rms and mean spectra (Kollatschny 2003b). The redshifted $\text{H}\alpha$ and $\text{H}\beta$ broad lines were found with the rms spectra for Seyfert 1 galaxy NGC 4593, and their redward shifts might be interpreted as the gravitational redshift (Kollatschny & Dietrich 1997). In this paper, we derive a new method to estimate the virial factors f with gravitationally redshifted broad optical emission lines in AGNs, and apply this new method to five reverberation mapped Seyfert 1 galaxies.

The structure of this paper is as follows. Section 2 presents the method. Section 3 describes the application to Mrk 110. Section 4 is for the application to NGC 4593. Section 5 is for the applications to Mrk 493, *IRAS* 04416 and Mrk 42. Section 6 presents discussion and conclusions. Throughout this paper, we use the standard cosmology with $H_0 = 70 \text{ km s}^{-1} \text{ Mpc}^{-1}$, $\Omega_{\text{M}} = 0.3$, and $\Omega_{\Lambda} = 0.7$ (Spergel et al. 2003; Riess et al. 2004).

2 METHOD

The BLRs are distant from the central black holes for the reverberation mapped AGNs. The Schwarzschild metric will be reasonable to describe the space-time around the BLRs. The Kerr metric and the Schwarzschild metric have the identical effect on the gravitational redshift at distances larger than about one hundred gravitational radii from the black holes (see Fig. 9 in Müller & Wold 2006). The Schwarzschild space-time is

$$\begin{aligned} ds^2 &= -g_{\mu\nu} dx^\mu dx^\nu \\ &= \left(1 - \frac{2GM_{\bullet}}{c^2 r}\right) c^2 dt^2 - \left(1 - \frac{2GM_{\bullet}}{c^2 r}\right)^{-1} dr^2 \\ &\quad - r^2 d\theta^2 - r^2 \sin^2 \theta d\varphi^2, \end{aligned} \quad (1)$$

where G is the gravitational constant, c is the speed of light, and M_{\bullet} is the mass of black hole. The ratio of the frequency

of atomic transition ν_e at the BLR radius r_{BLR} to the frequency ν_o observed at infinite distance is (static cloud)

$$\frac{\nu_o}{\nu_e} = \frac{(-g_{00})_{r_{\text{BLR}}}^{1/2}}{(-g_{00})_{\infty}^{1/2} c} = \left(1 - \frac{2GM_{\bullet}}{c^2 r_{\text{BLR}}}\right)^{1/2}, \quad (2)$$

where $(-g_{00})_{\infty} = 1$ at the observer's frame. So, the gravitational redshift is

$$z_g = \frac{\nu_e}{\nu_o} - 1 = \left(1 - \frac{2GM_{\bullet}}{c^2 r_{\text{BLR}}}\right)^{-1/2} - 1. \quad (3)$$

The black hole mass M_{\bullet} is

$$M_{\bullet} = \frac{1}{2} G^{-1} c^2 r_{\text{BLR}} [1 - (1 + z_g)^{-2}], \quad (4)$$

and the first order approximation is

$$M_{\bullet} \cong G^{-1} c^2 z_g r_{\text{BLR}}, \quad (5)$$

if $z_g \ll 1$. Equation (5) was used to estimate M_{\bullet} in Kollatschny (2003b) and Zheng & Sulentic (1990).

In general, the gravitational redshift z_g is derived from the redshift differences of the broad emission lines relative to the narrow emission lines. As the narrow lines do not appear in the spectrum containing the broad lines, the redshift differences $\Delta z_{i,j} = z_i - z_j = z_{g,i} - z_{g,j}$ for the broad lines i and j are used to estimate M_{\bullet} . And then we have

$$\Delta z_{i,j} = \left(1 - \frac{2GM_{\bullet}}{c^2 r_{\text{BLR},i}}\right)^{-1/2} - \left(1 - \frac{2GM_{\bullet}}{c^2 r_{\text{BLR},j}}\right)^{-1/2} \cong \frac{GM_{\bullet}}{c^2} \left(\frac{1}{r_{\text{BLR},i}} - \frac{1}{r_{\text{BLR},j}}\right), \quad (6)$$

where $r_{\text{BLR}} \gg r_g = GM_{\bullet}/c^2$ (r_g is the gravitational radius), and

$$M_{\bullet} \cong G^{-1} c^2 \Delta z_{i,j} \left(\frac{1}{r_{\text{BLR},i}} - \frac{1}{r_{\text{BLR},j}}\right)^{-1}, \quad (7)$$

where $r_{\text{BLR},i}$ and $r_{\text{BLR},j}$ correspond to the broad lines i and j , respectively. Black hole mass can be determined based on the virial theorem for the reverberation mapped AGNs:

$$M_{\text{RM}} = f \frac{v_{\text{FWHM}}^2 r_{\text{BLR}}}{G}, \quad (8)$$

where v_{FWHM} is the *FWHM* of broad emission line (Peterson et al. 2004). If both of the mapping method and the gravitational redshift method measure the mass M_{\bullet} , the mapping mass M_{RM} is equal to the gravitational redshift mass M_{grav} derived from equation (4) for each AGN. Thus, we have the virial factor

$$f = \frac{1}{2} \frac{c^2}{v_{\text{FWHM}}^2} [1 - (1 + z_g)^{-2}], \quad (9)$$

for the reverberation mapped AGNs. This gravitational redshift approach will be a terse method to estimate the virial factor f in equation (8). If the BLRs have disc-like geometry with an inclination θ , $f = 1/4 \sin^2 \theta$ (McLure & Dunlop 2001). As $f = 1$, $\theta = 30$ degrees.

3 APPLICATION TO MRK 110

The virial factor f is derived by equation (9) for broad lines He II, He I, H β and H α (see Table 1). Considering the errors of v_{FWHM} and z_g , the f distribution is generated with equation (9) by 10^4 realizations of Monte Carlo simulation. The mean and standard deviation of this distribution are regarded as the expectation and uncertainty of f , respectively. The helium and hydrogen lines have $f \approx 8$ –16 that are larger than the average $\langle f \rangle \approx 1$ usually accepted for the reverberation mapped AGNs. The f values of the helium lines are slightly smaller than those of the hydrogen lines. If the BLRs are disc-like, their inclination angles θ are ≈ 7 –10 degrees (see Table 1). These inclination angles indicate the nearly face-on view of the disc-like BLRs, and also confirm the nearly face-on view of accretion disc in Mrk 110 suggested by Kollatschny (2003a,b). The four broad lines He II, He I, H β and H α have obvious stratification in the BLRs, as predicted by the virial theorem (Kollatschny 2003b), and are from the near to the distant away from the central black hole. These stratification BLRs are dominated by the gravity of the central supermassive black hole. Mrk 110 will have the virial velocity $v_c^2 = GM_{\bullet} r_{\text{BLR}}^{-1}$ and $v_{\text{FWHM}}^2 \propto v_c^2 \propto r_{\text{BLR}}^{-1}$. We have $f \cong z_g c^2 / v_{\text{FWHM}}^2$ because $z_g \ll 1$ in equation (9) for Mrk 110, and then $f \propto z_g r_{\text{BLR}} \propto M_{\bullet}$ (see equation [5]). M_{\bullet} can be regarded as a constant in observation periods for individual AGNs. So, f is independent of r_{BLR} . However, there is a positive correlation between $\log f$ and $\log r_{\text{BLR}}$ for Mrk 110 (see Figure 1). This increasing trend of $\log f$ versus $\log r_{\text{BLR}}$ is inconsistent with the independent prediction of the virial theorem.

There are two paths to estimate black hole mass, i.e. the single broad-line estimation (equation [4]) and the broad-line-to-broad-line comparison (equation [7]). The mass M_{grav} is estimated for the broad lines He II, He I, H β and H α (see Tables 1 and 2). According to basic error propagation used conventionally in the reverberation mapping, we estimate the uncertainty of M_{grav} from the errors of r_{BLR} and z_g . Each M_{grav} value in Table 2 will correspond two M_{grav} values in Table 1 because equation (7) is based on two broad lines. Comparison between these two kinds of masses shows that the masses estimated by the two paths are consistent with each other (see Figure 2). This agreement indicates that the broad-line-to-broad-line comparison path is feasible and reliable to estimate M_{grav} . These black hole masses in Tables 1 and 2 are also consistent with the mean mass of $\log M_{\text{grav}}/M_{\odot} = 8.15$ derived in Kollatschny (2003b). The broad-line-to-broad-line comparison path is without the difficulty of the reference of the gravity redshift of broad line as in the single broad-line path, such as the blueshift of the narrow line [O III] $\lambda 5007$. This narrow line blueshift will generate equivalently a broad-line redshift as the blueshifted narrow line is used as the reference to estimate z_g . In principle, the broad-line-to-broad-line comparison path could eliminate mostly

Table 2. M_{grav} from broad lines for Mrk 110

Line (1)	He I $\lambda 5876$ (2)	H β $\lambda 4861$ (3)	H α $\lambda 6563$ (4)
He II $\lambda 4686$	8.10 ± 0.39	8.06 ± 0.28	8.08 ± 0.26
He I $\lambda 5876$		7.89 ± 0.66	8.02 ± 0.48
H β $\lambda 4861$			8.38 ± 0.82

Notes: gravitational masses derived from equation (7) and scaled as $\log \frac{M_{\text{grav}}}{M_{\odot}}$.

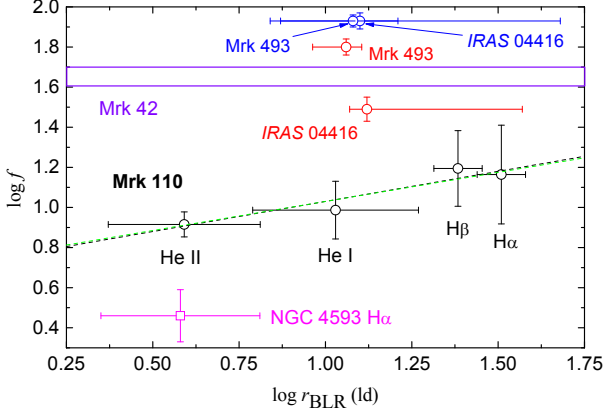


Figure 1. $\log f$ vs $\log r_{\text{BLR}}$. Black circles are for Mrk 110. Circles in color are for SEAMBH AGNs. Red circles denote the H β line, and blue circles denote the Fe II line. Violet lines denote the f values for Mrk 42. **Black line is the best fit to the black circles with a Pearson's correlation coefficient $r = 0.948$ at the confidence level of 94.8 percent [$y = 0.73(\pm 0.08) + 0.30(\pm 0.07) \times x$]. Green line is the best fit to the black circles and uncertainties in x and y by the "FITEXY" estimator (Press et al. 1992) with a chi-square $\chi^2 = 0.180$ and a goodness-of-fit $Q = 0.914$ [$y = 0.74(\pm 0.21) + 0.29(\pm 0.22) \times x$].**

the line shift influence due to the BLR "breath". In the terms of the two factors, this broad-line-to-broad-line comparison path seems to be better than the single broad-line path to estimate M_{grav} as there are several broad lines in spectra. So, equation (7) is appropriate to estimate M_{grav} for broad-line AGNs. Equation (4) is appropriate for a single broad line except for the blueshift issue of the narrow line used as the reference to estimate z_g .

4 APPLICATION TO NGC 4593

NGC 4593 is a nearby Seyfert 1 galaxy. This object is a sub-Eddington accretor with an average $\dot{\mathcal{M}} = 0.08$, where dimensionless accretion rate $\dot{\mathcal{M}} = \dot{M}_{\bullet}/L_{\text{Edd}}c^{-2}$ and \dot{M}_{\bullet} is the mass accretion rate (Du et al. 2015). Early reverberation mapping yielded a lag of four days indicating a very compact BLR (Dietrich et al. 1994). Recent reverberation mappings confirm this lag of four days (e.g. Du et al. 2015, references therein). Kollatschny & Dietrich (1997) found the redshifted H α and H β broad lines with the rms spectra, and thought that the observed redshift might be interpreted as the gravitational redshift. The central component of H α is redshifted by $110 \pm 30 \text{ km s}^{-1}$ and the H β rms spec-

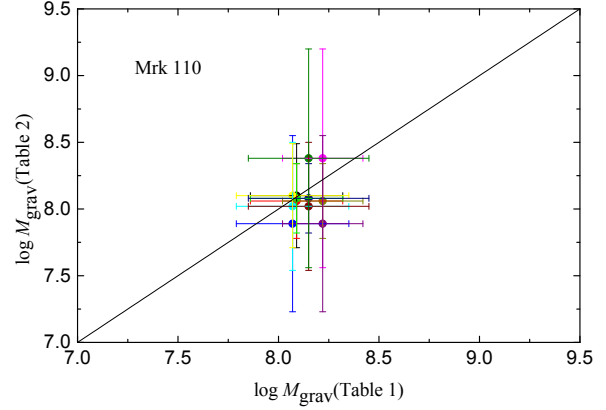


Figure 2. Comparison between M_{grav} derived from equations (4) and (7). Black line is $y = x$.

trum shows a redshift of the same order. We have $FWHM = 3400 \pm 200 \text{ km s}^{-1}$ for both of the H α rms and mean spectra. The relevant physical quantities of H α are listed in Table 1. A mass $M_{\text{grav}} = 2.5(\pm 1.5) \times 10^7 M_{\odot}$ is derived from equation (4). A value $f = 2.9$ is obtained for the redshifted H α line. This f value is slightly higher than the average $\langle f \rangle \approx 1$ usually accepted. The value $f = 2.9$ is smaller than those of Mrk 110. In plot of $\log f$ versus $\log r_{\text{BLR}}$, NGC 4593 is below the straight line best fit to Mrk 110 (see Figure 1). Mrk 110 has an average $\dot{\mathcal{M}} = 5.89$ (Du et al. 2015). The difference of position in plot of $\log f$ versus $\log r_{\text{BLR}}$ may be from the difference of $\dot{\mathcal{M}}$. If the BLR is disc-like in NGC 4593, the BLR inclination angle is ≈ 17 degrees. The inclination effect will generate different f even for the same disc-like BLR (e.g. McLure & Dunlop 2001). Another possible explanation of the different f is that the accretion rate $\dot{\mathcal{M}}$ dominates the factor f because both of $f = 2.9$ and $\dot{\mathcal{M}} = 0.08$ in NGC 4593 are smaller compared to both of $f = 14.6$ and $\dot{\mathcal{M}} = 5.89$ in Mrk 110 for H α . We have a normalization of $\dot{\mathcal{M}}$ relative to f $\dot{\mathcal{M}}_f = 0.03$ and 0.40 for NGC 4593 and Mrk 110, respectively. This normalized value $\dot{\mathcal{M}}_f$ reflects the composite effects of the central black hole gravity, the central radiation pressure and the kinematics and geometry of BLR. Mrk 110 has higher $\dot{\mathcal{M}}_f$ and f than does NGC 4593.

5 APPLICATIONS TO MRK 493, IRAS 04416 AND MRK 42

Hu et al. (2015) studied the properties of emission lines for 10 NLS1s. Mrk 493, IRAS 04416+1215 and Mrk 42 have the redward shifted optical Fe II and H β lines with respect to [O III] $\lambda 5007$. The virialized motions of BLR clouds are also assumed to estimate M_{RM} in the reverberation mapping of H β for these NLS1s (Du et al. 2014; Wang et al. 2014). So, the redward shifts of H β and Fe II may be the gravitational redshift. The Fe II lag is consistent with the H β lag for the same source (see Table 3). Mrk 493 and Mrk 42 have the Fe II $FWHM$ s indistinguishable from the H β $FWHM$ s. The Fe II $FWHM$ is slightly smaller than the H β $FWHM$ in IRAS 04416+1215.

Table 1. Virial factors, gravitational masses, and accretion disc inclinations of Mrk 110 and NGC 4593

Object	Line	$\frac{FWHM}{\text{km s}^{-1}}$	z_g	τ (days)	$\log \frac{M_{\text{grav}}}{M_{\odot}}$	f	θ°
(1)	(2)	(3)	(4)	(5)	(6)	(7)	(8)
Mrk 110	He II $\lambda 4686$	4444 ± 200	0.00180 ± 0.00020	3.9 ± 2	8.09 ± 0.23	8.23 ± 1.18	10.12 ± 0.74
Mrk 110	He I $\lambda 5876$	2404 ± 100	0.00062 ± 0.00020	10.7 ± 6	8.07 ± 0.28	9.70 ± 3.21	9.24 ± 1.56
Mrk 110	H β $\lambda 4861$	1515 ± 100	0.00039 ± 0.00017	24.2 ± 4	8.22 ± 0.20	15.65 ± 6.79	7.26 ± 1.68
Mrk 110	H α $\lambda 6563$	1315 ± 100	0.00025 ± 0.00017	32.3 ± 5	8.15 ± 0.30	14.59 ± 8.27	7.52 ± 2.79
NGC 4593	H α $\lambda 6563$	3400 ± 200	0.00037 ± 0.00010	3.8 ± 2.0	7.39 ± 0.26	2.91 ± 0.86	17.04 ± 2.60

Notes: Column 1: object names; Column 2: emission line names; Column 3: $FWHM$ s of broad emission lines in the rms spectra; Column 4: gravitational redshifts; Column 5: time lags of lines in the rest frame; Column 6: gravitational masses derived from equation (4); Column 7: the virial factors; Column 8: inclinations if BLRs have disc-like geometry.

It seems that there are no obvious stratification in BLRs for Mrk 493, *IRAS* 04416 and Mrk 42. Here, we regard these redward shifts of the Fe II and H β lines as the gravitational redshift. The details for these three NLS1s are listed in Table 3. The factors f and masses M_{grav} are estimated by equations (9) and (4), respectively. These three NLS1s have f higher than Mrk 110 (see Figure 1). The f values of these NLS1s are much larger than the average $\langle f \rangle \approx 1$ accepted usually in the reverberation mapping. The more high- f values imply that NLS1s may have higher black hole masses than M_{RM} in the case of $\langle f \rangle \approx 1$, and the higher masses will decrease the Eddington ratios. This is very similar to the case of Mrk 110 with a mean $f \approx 12$, which will make M_{RM} increase by an order of magnitude with respect to the mass estimated with $\langle f \rangle \approx 1$.

These NLS1s and Mrk 110 have comparable r_{BLR} and M_{grav} , but distinctly different f (see Figure 1). These behaviors might be from the difference between accretion states. Mrk 493 and *IRAS* 04416 have $\dot{M} = 75.9$ and $\dot{M} = 426.6$, respectively (Du et al. 2015). Mrk 493 and *IRAS* 04416 have a mean $f = 73.3$ and $f = 58.7$, respectively. Thus, Mrk 493 and *IRAS* 04416 have $\dot{M}_f = 1.04$ and $\dot{M}_f = 7.27$, respectively. Mrk 110 has a mean $f = 12.0$ and $\dot{M}_f = 0.49$. In terms of \dot{M} and \dot{M}_f , Mrk 493 and *IRAS* 04416 are at higher accretion states than Mrk 110. The higher accretion rate seems to correspond to the larger f . The higher accretion rate will produce the higher radiation pressure on the BLR clouds. The higher radiation pressure will counteract a more proportion of gravity of black hole, and then the BLR clouds will have a smaller virial velocity, i.e. v_{FWHM} will decrease if the radiation pressure increases, given that the BLR clouds are in virialized motions. Ultimately, the radiation pressure will influence M_{RM} . Thus, the factor f estimated by equation (9) will be higher than that expected from the virial assumption without considering the radiation pressure. If NLS1s have a disc-like BLR, there are inclinations of 3–5 degrees, indicating a nearly face-on view, for these three NLS1s.

A higher mass $\log M_{\text{grav}}/M_{\odot} \approx 9.5$ is estimated by equation (7) for *IRAS* 04416. A very large error of $\log M_{\text{grav}}/M_{\odot}$ will be generated by the larger error of τ ($r_{\text{BLR}} = c\tau$) (see Table 3). This larger mass is on the same order of magnitude as the mass estimated by equation (4) for Fe II when considering its errors. This means that the single broad-line path and the broad-line-to-broad-line compari-

son path are equally applicable to estimating M_{grav} for *IRAS* 04416. A further test is needed in the future with high quality time lags of H β and Fe II to check the validity of these two paths. The current result indicates that the redward shifts of H β and Fe II with respect to [O III] are reliable to be used as the gravitational redshift, i.e. the [O III] line redshift can be regarded as the systemic redshift. Equation (7) cannot be applied to Mrk 493. The applications to Mrk 110, *IRAS* 04416 and Mrk 493 show that the broad-line-to-broad-line comparison path is more applicable to those AGNs with obvious stratification in BLRs, such as Mrk 110.

6 DISCUSSION AND CONCLUSIONS

Müller & Wold (2006) used the Kerr ray tracing simulations to study the gravitational redshifts of Mrk 110. When $r_{\text{BLR}} \gtrsim 100 r_g$, the simulation results for stationary rotating emitters are nearly identical to, within the errors, those for static emitters in the Kerr space-time and the Schwarzschild space-time (see Fig. 9 in Müller & Wold 2006). Mrk 110 has $r_{\text{BLR}} \sim 560\text{--}4000 r_g$ for the broad lines He II, He I, H β and H α . So, it is reasonable and reliable to estimate f and M_{grav} by using the formulas in section 2. The gravitational redshift effect will exist in the broad lines as long as the BLRs in AGNs surround the central supermassive black holes. However, the gravitational redshift is not always observable due to several factors. The first factor is the observational accuracies, such as the low signal to noise ratios. The second is the breathing of BLRs that shifts the broad lines redward or blueward. The rms and mean spectra may eliminate this breathing effect of BLRs on z_g . The rms and mean spectra were used to measure z_g of the broad lines in Mrk 110 (Kollatschny 2003b) and NGC 4593 (Kollatschny & Dietrich 1997). The third is that the inflow can also produce the broad line redward shifts relative to the narrow lines. The reverberation mapping assumes that the BLR cloud motions meet the virial theorem. It was ruled out that radial inflow or outflow motions are dominant in the BLRs of NGC 4593 (Kollatschny & Dietrich 1997), Mrk 110 (Kollatschny 2003a), Mrk 50 (Barth et al. 2011) and Mrk 1044 (Du et al. 2016). The fourth is the other broad and/or narrow lines blended with the target broad line, which may make z_g unobservable. These blended line components will influence the $FWHM$ and centroid of broad line in the rms spectra (e.g. Barth et al. 2015). So, these blended line

Table 3. Virial factors, masses, and accretion disc inclinations of NLS1s derived from H β and Fe II lines

Object	Line	$\frac{FWHM}{\text{km s}^{-1}}$	z_g	τ (days)	$\log \frac{M_{\text{grav}}}{M_{\odot}}$	f	θ°
(1)	(2)	(3)	(4)	(5)	(6)	(7)	(8)
<i>IRAS</i> 04416+1215	H β	1522 \pm 44	0.00080 \pm 0.00010	13.3 $^{+13.9}_{-1.4}$	8.27 $^{+0.46}_{-0.07}$	31.14 \pm 4.29	5.14 \pm 0.37
Mrk 42	H β	802 \pm 18	0.00029 \pm 0.00006			40.60 \pm 8.60	4.50 \pm 0.55
Mrk 493	H β	778 \pm 12	0.00042 \pm 0.00004	11.6 $^{+1.2}_{-2.6}$	7.93 $^{+0.06}_{-0.11}$	62.44 \pm 6.26	3.63 \pm 0.19
<i>IRAS</i> 04416+1215	Fe II	1313 \pm 50	0.00165 \pm 0.00007	12.6 $^{+16.7}_{-6.7}$	8.56 $^{+0.58}_{-0.23}$	86.31 \pm 7.56	3.09 \pm 0.14
Mrk 42	Fe II	787 \pm 16	0.00035 \pm 0.00006			50.94 \pm 8.97	4.02 \pm 0.38
Mrk 493	Fe II	780 \pm 9	0.00057 \pm 0.00003	11.9 $^{+3.6}_{-6.5}$	8.08 $^{+0.13}_{-0.24}$	84.25 \pm 4.85	3.12 \pm 0.09

Notes: Same as in Table 1 except for Column 3: the H β line $FWHM$ s are from the mean spectra and the Fe II line $FWHM$ s are the means and standard deviations obtained from the measurements of individual-night spectra (Hu et al. 2015).

components may make it difficult to measure z_g in the single-epoch spectra. If several broad lines in the single-epoch spectrum have z_g of the same order of magnitude, their z_g may be reliable. For example, Q1011+250, Q1630+377 and Q1634+70 have $z_g = 0.004$, 0.004 and 0.006 for H β , respectively (Nishihara et al. 1997). Also, three are $z_g = 0.004$, 0.006 and 0.005 for H α , respectively. This multi-broad-line approach may be reliable to obtain z_g from the single-epoch spectra for quasars. It may improve the statistical researches on z_g in quasars.

In the absence of the radiation pressure on the BLR clouds of AGNs with masses M_{\bullet} , there is $v_c^2 = GM_{\bullet}/r_{\text{BLR}} = r_{\text{BLR}}^{-1}(r_g)c^2$, where $r_{\text{BLR}}(r_g)$ is in units of r_g . At the same time, $v_{\text{FWHM}}^2 \propto v_c^2 \propto r_{\text{BLR}}^{-1}(r_g)$. Equations (4) and (9) are combined to give $f = GM_{\bullet}/(r_{\text{BLR}}v_{\text{FWHM}}^2) \propto r_{\text{BLR}}^{-1}(r_g)/v_{\text{FWHM}}^2 \propto C$, where C is independent of r_{BLR} and M_{\bullet} . However, Figure 1 shows the evidence of the increasing trend of f with r_{BLR} . So, this problem may result from the ignoring of the radiation pressure of accretion disc on these clouds. The radiation pressure will push these clouds towards the larger radius compared to the BLR radius in the absence of the radiation pressure. Thus, $v_c^2 \neq GM_{\bullet}/r_{\text{BLR}}$ in the presence of the radiation pressure. We will have $v_{\text{cr}}^2 = GM_{\bullet}/r_{\text{BLR}}/(r_{\text{BLR}}/ld)^{\alpha}$ instead of $v_c^2 = GM_{\bullet}/r_{\text{BLR}}$ for AGNs with luminous accretion discs, where $(r_{\text{BLR}}/ld)^{-\alpha}$ is the correction factor due to the central disc radiation and $\alpha > 0$. So, $v_{\text{cr}}^2 < v_c^2$ for the same radius r_{BLR} , and $v_{\text{FWHM}}^2 \propto v_{\text{cr}}^2 \propto r_{\text{BLR}}^{-1}(r_g)(r_{\text{BLR}}/ld)^{-\alpha}$. Thus, $f \propto r_{\text{BLR}}^{-1}(r_g)/v_{\text{FWHM}}^2 \propto (r_{\text{BLR}}/ld)^{\alpha}$, i.e. $\log f = D + \alpha \log(r_{\text{BLR}}/ld)$, where D is independent of r_{BLR} and M_{\bullet} . The virial factor f is a function of r_{BLR} rather than $r_{\text{BLR}}(r_g)$. α is likely different from one to another AGN and might depend on accretion rates. We have $\alpha \approx 0.3$ for Mrk 110 (see Figure 1). The lines in parallel with the best fit straight line to Mrk 110 cannot connect two points of Mrk 493 or *IRAS* 04416 even considering the corresponding errors. It is obvious that a larger α is needed to connect the two points of Mrk 493 or *IRAS* 04416. Mrk 110, Mrk 493 and *IRAS* 04416 have $\mathcal{M} = 5.89$, 75.9 and 426.6 or $\mathcal{M}_f = 0.49$, 1.04 and 7.27, respectively. Then, Mrk 493 and *IRAS* 04416 have larger α and accretion rates than Mrk 110 has, i.e. α likely depends on accretion rate. The virial factor f is an increasing function of r_{BLR} , and this increasing trend results from the radiation pressure influence on the BLR clouds due to the central accretion disc radiation. For individual AGNs, the radiation pressure due to accretion disc will produce more obvious effect on the BLR

clouds as α increases. As α vanishes, the radiation pressure effect also vanishes. These larger f values ≈ 8 –16 will make M_{RM} increase for Mrk 110, with respect to the mass derived from $\langle f \rangle \approx 1$. In like manner, the largening of f may exist in quasars. Quasar J0100+2802 at $z = 6.30$, the most luminous quasar known at $z > 6$, has a black hole mass of ~ 12 billion M_{\odot} and a bolometric luminosity of 1.62×10^{48} ergs s $^{-1}$ (Wu et al. 2015). The largening of f will give a larger mass in J0100+2802. The larger black hole mass further gives rise to the most significant challenge to the Eddington limit growth of black holes in the early Universe (Volonteri 2012; Willott et al. 2010). The larger f values than $\langle f \rangle \approx 1$ will decrease the Eddington ratios. The lower Eddington ratios will set constraints on accretion states.

The redward shift of broad line relative to [O III] $\lambda 5007$ also may arise from a velocity-origin, either the broad-line cloud inflow towards the central black hole (e.g. McIntosh et al. 1999b; Hu et al. 2015), or the [O III] $\lambda 5007$ emitting cloud outflow (e.g. Boroson 2005; Bae & Woo 2014; Zhou et al. 2006). Boroson (2005) and Zhou et al. (2006) estimated the velocity offset of [O III] $\lambda 5007$ relative to the low-ionization lines [O II], [N II] and/or [S II]. However, the [O II] lines are redshifted or blueshifted relative to the [N II] and [S II] doublets (Zhou et al. 2006). Also, the [N II] and [O III] $\lambda 5007$ show the redshifted and blueshifted cases with respect to the stellar absorption lines (Bae & Woo 2014). A mean shift of -40 km s $^{-1}$ was obtained for [O III] (the minus denotes blueshift) (Boroson 2005). Zhou et al. (2006) found a mean shift of ~ -40 km s $^{-1}$, ~ -20 km s $^{-1}$ and \sim zero for [O III], the broad component of H β and the broad component of H α , respectively, in ~ 2000 NLS1s. Moreover, the narrow line shifts have a wider range on the order of magnitude of 100 km s $^{-1}$. Thus, there are some problems in estimating the shift of emission line relative to narrow line with the single-epoch spectrum for individual AGNs. The broad-line-to-broad-line comparison path (equation[7]) will overcome the limitations of narrow line shifts. The single broad-line path (equation [4]) is of problem of the narrow line shifts, and this problem may be avoided in the rms and mean spectra. Comparisons between M_{grav} of Mrk 110 derived from the broad-line-to-broad-line comparison path and the single broad-line path show that the rms and mean spectra could overcome the limitations of narrow line shifts. The redward shifts of

broad lines could be from the BLR cloud inflow, and this explanation seems to be easily understood except that some extra parameters are needed to describe the inflow. Jonić et al. (2016) found significant positive correlations between intrinsic shift Δz_{50} and v_{FWHM} of broad $\text{H}\beta$ and Mg II , $\Delta z_{50} \propto v_{\text{FWHM}}^n$ with $n \approx 2$, for AGNs. These correlations confirm the gravitational redshift origin of the relevant redward shifts. The gravitational redshift is a natural outcome of virialized motions of BLR clouds in AGNs. The blueshift is usually obtained for high-ionization broad lines, e.g. C IV (e.g. Wang et al. 2011, references therein). The blueshift is difficult to reconcile with gravitationally-bound BLR models, but is considered as a signature of gas outflow that is a natural interpretation of blueshift of high-ionization lines (e.g. Wang et al. 2011, references therein). The outflow is driven by the radiation pressure of the central accretion disc. The blueshifts of $\text{H}\beta$ and Fe II are also found for the reverberation mapped NLS1s in Hu et al. (2015), and can be explained as the BLR cloud outflow driven by the radiation pressure. The redward redshifts of $\text{H}\beta$ and Fe II are likely the gravitational redshift of clouds in virialized motions due to the central supermassive black holes in NLS1s.

IRAS 04416 and Mrk 493 have a mean $r_{\text{BLR}} \sim 900r_g$ and $\sim 2000r_g$, respectively. According to Müller & Wold (2006), the gravitational redshift can be probed out to $r_{\text{BLR}} \sim 900r_g$ and $\sim 2000r_g$ with a resolution of $\approx 8.3 \text{ \AA}$ and $\approx 3.8 \text{ \AA}$, respectively. The spectra measured in the reverberation mapping campaign for SEAMBHs have a resolution of 1.8 \AA (Du et al. 2014; Hu et al. 2015). Thus, the gravitational redshift can be probed out to $r_{\text{BLR}} \sim 900r_g$ and $\sim 2000r_g$, respectively, for *IRAS* 04416 and Mrk 493 with the spectra used to measure the redward shifts of $\text{H}\beta$ and Fe II . The spectral resolution of $\sim 500 \text{ km s}^{-1}$ mentioned in Du et al. (2014) and Hu et al. (2015) is an instrumental broadening that mainly influences width of spectrum line, such as *FWHM*, but slightly influences the central wavelength of spectrum line. The instrumental broadening has been corrected to obtain *FWHMs* of broad lines in NLS1s (Du et al. 2014; Hu et al. 2015). On the basis of the ultraviolet reverberation mapping of carbon lines, a small inclination angle is suggested, supporting a high- f value, for PG 1247+267, the brightest quasar ever analyzed for reverberation with $\lambda L_{\lambda}(1350\text{\AA}) = 3.9 \times 10^{47} \text{ ergs s}^{-1}$ and ionization stratification similar to low-luminosity AGNs (Trevese et al. 2014). There is a redward shift of 0.008 for broad $\text{H}\beta$ with respect to $[\text{O III}] \lambda 5007$ in the infrared spectrum (McIntosh et al. 1999b). The broad $\text{H}\beta$ has $v_{\text{FWHM}} = 7460 \text{ km s}^{-1}$ (McIntosh et al. 1999a). Assuming the shift of 0.008 is the gravitational redshift, we have $f \approx 13$. An inclination angle ≈ 8 degrees is derived for PG 1247+267 if the $\text{H}\beta$ BLR has a disc-like geometry. Our results are consistent with those in Trevese et al. (2014). This indicates that the gravitational redshift of $\text{H}\beta$ is reliable on the order of magnitude for PG 1247+267, and the new method is feasible to estimate f in quasars. Mrk 110, and other three NLS1s and PG 1247+267 have high- f values and small inclinations of BLRs. It seems that the gravitationally redshifted optical spectrum

lines are more easily detected in the AGNs with the nearly face-on viewed BLRs, due to the fact that the competing Doppler effect is weaker than the gravitational redshift effect in the case of the nearly face-on disc-like BLRs (e.g. Müller & Wold 2006).

In this paper, based on the gravitationally redshifted optical broad emission lines in AGNs, a new method is proposed to measure the virial factors f in M_{RM} by using z_g and v_{FWHM} of broad lines. It is difficult to determine f in the reverberation mapping due to the unclear kinematics and geometry of BLRs in AGNs. The different f implies the difference of geometry and kinematics of the BLRs. First, this new method is applied to NLS1 Mrk 110 with the gravitationally redshifted broad lines He II , He I , $\text{H}\beta$ and $\text{H}\alpha$. These four lines have $f \approx 8\text{--}16$ that are distinctly larger than the mean $\langle f \rangle \approx 1$ derived from the $M_{\bullet} - \sigma_{\star}$ relation. The He II and He I lines have slightly smaller f than do the $\text{H}\beta$ and $\text{H}\alpha$ lines. There is a positive correlation between the factor f and the radius r_{BLR} for Mrk 110 (see Figure 1), and this increasing trend can be naturally explained by the radiation pressure influence of accretion disc on the BLR clouds in Mrk 110. The radiation pressure influence seems to be more important than thought usually in AGNs. Second, Seyfert 1 NGC 4593 has $f = 2.9$ derived from the redshifted $\text{H}\alpha$ line. Third, NLS1s Mrk 493, *IRAS* 04416 and Mrk 42 have high- f values of several tens derived from the redward shifted optical $\text{H}\beta$ and Fe II lines. In plot of $\log f$ versus $\log r_{\text{BLR}}$, NGC 4593 is below the line best fit to Mrk 110, and both of Mrk 493 and *IRAS* 04416 are above the same line. This difference may result from accretion rate difference. NGC 4593, Mrk 110, Mrk 493 and *IRAS* 04416 have $\dot{M} = 0.08, 5.89, 75.9$ and 426.6 or $\dot{M}_{\text{f}} = 0.03, 0.49, 1.04$ and 7.27 , respectively. Also, the factor f increases for these four objects. The higher accretion rate may correspond to the larger f in different AGNs. The larger f of four NLS1s suggest the nearly face-on viewed BLRs if their BLRs have a disc-like geometry. The measurements of f from the gravitationally redshifted optical broad lines have the potential to improve M_{RM} . This paper is based on the condition that the optical BLRs are at the distances of hundreds to thousands of r_g away from the central black holes. NGC 4593, Mrk 110, Mrk 493 and *IRAS* 04416 have $r_{\text{BLR}} \sim 2700 r_g, 560\text{--}4000 r_g, 1700\text{--}2400 r_g$ and $600\text{--}1300 r_g$, respectively. So, this condition is met and the Schwarzschild metric is applicable to deducing the formulas in section 2. These larger f values derived from the gravitational redshift method can generate the higher black hole masses and the lower Eddington ratios with respect to those in the case of $\langle f \rangle \approx 1$ for AGNs.

ACKNOWLEDGMENTS

We are grateful to the anonymous referee for important comments leading to significant improvement of this paper. We thank the helpful discussions of Dr. H. Q. Li, Dr. P. Du and Dr. F. Wang. HTL thanks the National Natural Science Foundation of China (NSFC; grants 11273052 and U1431228) for financial support. JMB acknowledges the support of the NSFC (grant 11133006). HTL also thanks the financial supports of the project of the Training Pro-

gramme for the Talents of West Light Foundation, CAS and the Youth Innovation Promotion Association, CAS.

REFERENCES

- Bae H. J., Woo J. H., 2014, *ApJ*, 795, 30
- Barth A. J. et al., 2011, *ApJ*, 743, L4
- Barth A. J. et al., 2015, *ApJS*, 217, 26
- Bentz M. C. et al., 2006, *ApJ*, 651, 775
- Blandford R. D., McKee C. F., 1982, *ApJ*, 255, 419
- Boroson T., 2005, *AJ*, 130, 381
- Carswell R. F. et al., 1991, *ApJ*, 381, L5
- Denney K. D. et al., 2010, *ApJ*, 721, 715
- Dietrich M. et al., 1994, *A&A*, 284, 33
- Du P. et al. (SEAMBH Collaboration), 2014, *ApJ*, 782, 45
- Du P. et al. (SEAMBH Collaboration), 2015, *ApJ*, 806, 22
- Du P. et al. (SEAMBH Collaboration), 2016, *ApJ*, 820, 27
- Fabian A. C., Rees M. J., Stella L., White N. E., 1989, *MNRAS*, 238, 729
- Fabian A. C., Iwasawa K., Reynolds C. S., Young A. J., 2000, *PASP*, 112, 1145
- Haas M., Chini R., Ramolla M., Pozo Nuñez, F., Westhues C., Watermann R., Hoffmeister V., Murphy M., 2011, *A&A*, 535, A73
- Hu C. et al. (SEAMBH Collaboration), 2015, *ApJ*, 804, 138
- Jonić, S., Kovačević-Dojčinović, J., Ilić, D., Popović, L. Č., 2016, *Ap&SS*, 361, 101
- Kaspi S., Netzer H., 1999, *ApJ*, 524, 71
- Kaspi S., Smith P. S., Netzer H., Maoz D., Jannuzi B. T., Givon U., 2000, *ApJ*, 533, 631
- Kaspi S., Brandt W. N., Maoz D., Netzer H., Schneider D. P., Shemmer O., 2007, *ApJ*, 659, 997
- King A. L. et al., 2015, *MNRAS*, 453, 1701
- Kollatschny W., Dietrich M., 1997, *A&A*, 323, 5
- Kollatschny W., Bischoff K., Robinson E. L., Welsh W. F., Hill G. J., 2001, *A&A*, 379, 125
- Kollatschny W., 2003a, *A&A*, 407, 461
- Kollatschny W., 2003b, *A&A*, 412, L61
- Krolik J. H., Horne K., Kallman T. R., Malkan M. A., Edelson R. A., Kriss G. A., 1991, *ApJ*, 371, 541
- Krolik J. H., 2001, *ApJ*, 551, 72
- McIntosh D. H., Rieke M. J., Rix H. W., Foltz C. B., Weymann R. J., 1999a, *ApJ*, 514, 40
- McIntosh D. H., Rix H. W., Rieke M. J., Foltz C. B., 1999b, *ApJ*, 517, L73
- McLure R. J., Dunlop J. S., 2001, *MNRAS*, 327, 199
- Müller A., Wold M., 2006, *A&A*, 457, 485
- Nishihara E., Yamashita T., Yoshida M., Watanabe E., Okumura S., Mori A., Iye M., 1997, *ApJ*, 488, L27
- Onken C. A., Ferrarese L., Merritt D., Peterson B. M., Pogge R. W., Vestergaard M., Wandel A., 2004, *ApJ*, 615, 645
- Pei L. et al., 2014, *ApJ*, 795, 38
- Peterson B. M., 1993, *PASP*, 105, 247
- Peterson B. M. et al., 2004, *ApJ*, 613, 682
- Peterson B. M. et al., 2005, *ApJ*, 632, 799
- Piotrovich M. Y., Gnedin Yu. N., Silant'ev N. A., Natsvlshvili T. M., Buliga S. D., 2015, *MNRAS*, 454, 1157
- Popovic L. C., Vince I., Atanackovic-Vukmanovic O., Kubicela A., 1995, *A&A*, 293, 309
- Pozo Nuñez, F., Ramolla M., Westhues C., Bruckmann C., Haas M., Chini R., Steenbrugge K., Murphy M., 2012, *A&A*, 545, A84
- Press W. H., Teukolsky S. A., Vetterling W. T., Flannery B. P. 1992, *Numerical Recipes* (2nd ed.; Cambridge: Cambridge Univ. Press)
- Rees M. J., 1984, *ARA&A*, 22, 471
- Rees M. J., Begelman M. C., Blandford R. D., Phinney E. S., 1982, *Nature*, 295, 17
- Reynolds C. S., Nowak M. A., 2003, *Phys. Rep.*, 377, 389
- Riess A. G. et al., 2004, *ApJ*, 607, 665
- Shen Y. et al., 2015a, *ApJS*, 216, 4
- Shen Y. et al., 2015b, *ApJ*, 805, 96
- Shen Y. et al., 2016, *ApJ*, 818, 30
- Spergel D. N. et al., 2003, *ApJS*, 148, 175
- Tanaka Y. et al., 1995, *Nature*, 375, 659
- Tremaine S., Shen Y., Liu X., Loeb A., 2014, *ApJ*, 794, 49
- Trevese D., Perna M., Vagnetti F., Saturni F. G., Dadina M., 2014, *ApJ*, 795, 164
- Vanden Berk, D. E. et al., 2001, *AJ*, 122, 549
- Volonteri M., 2012, *Science*, 337, 544
- Wandel A., Peterson B. M., Makkan M. A., 1999, *ApJ*, 526, 579
- Wang H. Y. et al., 2011, *ApJ*, 738, 85
- Wang J. M. et al. (SEAMBH Collaboration), 2014, *ApJ*, 793, 108
- Willott C. J. et al., 2010, *AJ*, 140, 546
- Woo J. H., Urry C. M., 2002, *ApJ*, 579, 530
- Woo J. H., Yoon Y., Park S., Park D., Kim S. C., 2015, *ApJ*, 801, 38
- Wu X. B. et al., 2015, *Nature*, 518, 512
- Zheng W., Sulentic J. W., 1990, *ApJ*, 350, 512
- Zhou H. Y. et al., 2006, *ApJS*, 166, 128